CHAPTER VII

INFLUENCE OF POLYETHYLENE OXIDE ON THE RHEOLOGICAL PROPERTIES OF SEMI-DILUTE, WORMLIKE MICELLAR SOLUTIONS OF HEXADECYLTRIMETHYLAMMONIUM CHLORIDE AND SODIUM SALICYLATE

7.1 Abstract

The influence of polyethylene oxide (PEO) on the rheological properties of equimolar wormlike micellar solutions of, hexadecyltrimethylammonium chloride (HTAC) and sodium salicylate (NaSal) is investigated, above the concentration where a micellar entanglement network is formed. PEO is known to have a temperature-dependent binding affinity for HTAC micelles. The influence of temperature, PEO concentration, and HTAC concentration is explored. Within the concentration and temperature range examined (25 -100 mM HTAC and 25-50°C), HTAC/NaSal solutions exhibit rheological characteristics of an entanglement network. Application of transient network theory provides information in the form of the plateau modulus, G'_{∞}, the terminal viscoelastic relaxation time, τ_R, the reptation time, τ_{rep}, the micellar breaking time, τ_{br}, the mean micellar length, $\overline{L}$, and the entanglement length, l_e. Consistent with literature data, increase of HTAC concentration results in an evolution from slow-breaking to fast-breaking behavior, accompanied by an increase in G'_{∞} and τ_{rep}, and decreases in τ_R, and τ_{br}, l_e and $\overline{L}$. Addition of PEO results in a substantial decrease in G'_{∞} (increase in l_e), and corresponding increases in τ_R, and $\overline{L}$. These observations are consistent with the idea that binding of HTAC micelles to PEO in aqueous solution decreases the number of surfactant molecules available to contribute to the entanglement network of wormlike micelles.

7.2 Introduction

The influence of polymer-surfactant interactions on solution rheology is not only of scientific interest but also of industrial importance, since products ranging from paints to lubricants and cosmetic formulations consist of such mixtures [1]. In the last two decades, the rheological properties of aqueous solutions containing cationic surfactant with different kinds of binding counterions have been studied extensively [2-14]. Combination of a cationic surfactant, such as HTAB or hexadecyltrimethylammonium chloride (HTAC), with a strongly-binding counterion, such as sodium salicylate (NaSal), facilitates formation of long wormlike or threadlike micelles, 2-5 nm in diameter and 15-20 nm in persistence length, l_p, by screening the electrostatic repulsions between the charged surfactant head groups [7]. Semi-dilute solutions of such micelles exhibit highly non-Newtonian and viscoelastic behavior characteristic of entanglement network formation [2-14]. Like their polymer counterparts, entangled solutions of wormlike micelles can function as thickening and rheological control agents. The relaxation theories for entangled polymers are applicable to solutions of wormlike micelles, provided they are modified to reflect the fact that the flexible wormlike micelle can break and recombine continuously.

Cates et al. [15-19] proposed a model for micellar networks or living polymers incorporating the two competing dynamical processes, viz. reptation of wormlike micelles (with characteristic relaxation time τ_{rep}), and breaking and reconnecting of the micellar units (with characteristic relaxation time τ_{br}). In the fast breaking limit ($\tau_{br} << \tau_{rep}$), the Cates model predicts the stress relaxation is described by a single exponential decay with a relaxation time [15-18]:

$$\tau_R = \left(\tau_{br} \cdot \tau_{rep}\right)^{\frac{1}{2}} \qquad (1)$$

and zero shear viscosity (η_o) related to the plateau modulus (G_o) by:

$$\eta_0 = G_o \tau_R \qquad (2)$$

The frequency-dependent shear moduli are described by the Maxwell model:

$$G' = \frac{G_0 \omega^2 \tau_R^{\,2}}{1+\omega^2 \tau_R^{\,2}} \tag{3}$$

and

$$G'' = \frac{G_0 \omega \tau_R}{1+\omega^2 \tau_R^{\,2}} \tag{4}$$

The plateau modulus, G_o and the stress relaxation time, τ_R can therefore be deduced, respectively from the modulus value and crossover frequency, ω_c at the intersection point: $G'(\omega_c) = G''(\omega_c) = G_o/2$, and $\omega_c = 1/\tau_R$. In the slow breaking limit, ($\tau_{rep} \approx \tau_{br}$), which, from equation 3, implies that $\tau_R \sim \tau_{rep} \sim \tau_{br}$, the stress relaxation function exhibits a non-exponential decay. Granek and Cates [19] further included the contribution of breathing and Rouse motions of chain segments smaller than the entanglement spacing, to describe the short-time stress relaxation function. In this non-exponential dynamical regime, the true plateau modulus, G'_∞, is generally larger than that (G_o) determined via a fit of the low-frequency moduli to the Maxwell model.

The influence of these distinct dynamical processes is most easily visualized in a Cole-Cole plot of the loss modulus, G", versus the storage modulus, G' [15-19]. At low frequencies ($\omega\tau_R << 1$), entangled solutions of wormlike micelles show Maxwell behavior, as manifested in a semicircular Cole-Cole plot. A deviation from the semicircular Cole-Cole plot occurs at a frequency $\omega \approx \tau_{br}^{-1}$. The presence of breathing and Rouse modes is revealed by an upturn in the Cole-Cole plot at high frequencies, characteristic of molecular motions between entanglements ($\omega\tau_{br} >> 1$). From the analysis of Granek and Cates [19], the value of G" at the dip (G''_{min}) in the Cole-Cole plot is given by

$$\frac{G''_{min}}{G'_\infty} = A\frac{l_e}{\bar{L}} \tag{5}$$

where A is a constant of order unity, l_e is an entanglement length associated with the Rouse time, and $\bar{L}$ is the average micellar length. The entanglement length can be determined from the true plateau modulus, G'_∞ [19]:

$$G_{\infty}^{'} = \frac{k_B T}{l_e^{9/5} l_p^{6/5}} \tag{6}$$

where k_B is the Boltzmann constant, T is absolute temperature, and l_p is the persistence length of the micelle.

While it is well-known that strong binding interactions can exist between water-soluble polymers and surfactant micelles, driven by hydrophobic association, relatively few studies have attempted to explore the influence of such interactions on the rheology of semi-dilute solutions, and these appear to be confined entirely to hydrophobically-modified self-associating polymers [20]. In such systems addition of the polymer appears to enhance the viscosity and elasticity of the micellar solutions [20]. It is therefore of interest to determine whether a non-associative polymer such as polyethylene oxide (PEO), also known to complex with cationic micelles through hydrophobic interactions [21-24], will similarly modify the viscoelastic behavior of wormlike micellar solutions, formed by combining the cationic polymer with a binding counterion.

In the present paper, we explore the influence of addition of small amounts of PEO on the rheological behavior of semidilute equimolar solutions of hexadecyltrimethylammonium chloride (HTAC) and the binding salt NaSal. This study is stimulated by the observations of Khine *et al.* [22, 23] and Suksamranchit *et al* [24] who demonstrated that PEO forms complexes with HTAC, in which the surfactant micelles are bound to the polymer. The driving force for this complex formation appears to be hydrophobic interactions which are enhanced by increasing temperature. Our aim is to explore whether such interactions may influence the viscoelastic behavior of entangled solutions of wormlike HTAC/NaSal micelles. Three potential outcomes seem possible: (i) binding interactions of PEO with the HTAC micelles act as additional crosslinks, increasing the elasticity of the solution; (ii) complex formation between HTAC and PEO removes HTAC from the HTAC/NaSal network resulting in a decrease in the solution elasticity; (iii) no interaction occurs, in which case the micellar network elasticity remains unchanged,

and one observes a modest increase in solution viscosity due to the added PEO. Our results will favor the second of these possibilities.

The rheological properties of equimolar solutions containing HTAB and NaSal have been studied, and indeed show features (non-Newtonian viscosity and elasticity) characteristic of an entanglement network of wormlike micelles [4-10]. Experimental data on these solutions are presented here as a benchmark to exhibit the effect on the rheology of addition of the water soluble polymer polyethylene oxitle (PEO).The effects of temperature, polymer and surfactant concentrations on solution rheology of HTAC/NaSal solutions with and without PEO were investigated systematically. The results are interpreted within the framework of the Cates model [15-19], to provide information on the effect of PEO-surfactant interaction on the characteristic parameters: G_o, G'_{∞}, η_o, τ_R, τ_{rep}, τ_{br}, $\bar{L}$ and l_e.

7.3 Experimental

The surfactant used in this work is hexadecyltrimethylammonium chloride (HTAC) purchased from Fluka (purum $\geq$ 98.0 %). Sodium salicylate (NaSal) or 2-Hydroxybenzoic acid sodium salt (99%) was used as the counterion and purchased from Alfa Aesar (Johnson Matthey). Nonionic water soluble polymer, poly(ethylene oxide), PEO, with a quoted average molecular weights of 1.0×10^5 g/mol (Aldrich Chemical Co.) was used as received. The molecular weights of HTAC and NaSal are 319.5 and 160.1 g/mol, respectively. The sample solutions were prepared by dissolving appropriate amounts of HTAC, NaSal and PEO in deionized water (prepared by gravity filtration through Millipore filters, FHLP 01300; pore size 0.5 μm). Before measurements, all sample solutions were stored at room temperature for at least 24 hours to attain the equilibrium condition.

The rheological measurements were taken by a controlled strain fluid rheometer (Rheometrics, model ARES V6.5.6.). A cone and plate fixture was used with a cone diameter of 25 mm and a cone angle of 0.04 rad. A gap was set at 0.051 mm. The transducer sensitivity was between 0.004 – 10.00 g-cm. All experiments were measured using the log frequency-sweep test at a given strain (γ) chosen in the

linear viscoelastic regime, where the dynamic moduli are independent of strain. The frequency was varied from 0.01 to 100 rad/s. A steady shear sweep test was also carried out to determine the zero shear viscosity of sample solutions at different temperatures. The applied shear rate was varied from 0.1 to 1000 s^{-1}. The solution temperature was controlled by a circulating temperature bath and set at 30°C. Fresh surfactant solutions were used in each measurement to avoid evaporation of the solvent. After loading, each sample solution was left to equilibrate for about 10 min prior to measurement.

Data Analysis

It is known [25,26] that in general one cannot self-consistently fit the frequency-dependent moduli to theoretical Cole-Cole plots that include the nonreptative high-frequency effects, and so it is preferable to analyse the data via theory which excludes such effects. The true plateau modulus, G'_∞, is estimated by extrapolation of the Cole-Cole plots at high frequency to intercept the horizontal axis. The ratio, $\bar{\zeta} = \tau_{br}/\tau_R$, is then calculated from the reduced diameter of the fitted semicircle, DFS $\equiv G_o/G'_\infty$, via the graphical plot given by Turner and Coles [18]. Next, from $\bar{\zeta}$, τ_{br} is obtained using the experimental value of τ_R, and then τ_{rep} is calculated via equation (1). Subsequently, the average entanglement length, l_e, can be obtained from G'_∞ via equation (6). Here, we set the micellar persistence length l_p = 15 nm, which is a literature value for HTAB micelles [19]. The average micellar length, $\bar{L}$ can then be estimated, following Granek and Cates [19], from equation (5), with the assumption that A = 1. Values of the zero-shear viscosity were obtained by extrapolation either from low-frequency moduli or from low steady-shear viscosity measurements.

7.4 Results

Figures 1a and 1b illustrate the effect of temperature on the rheological behavior of equimolar aqueous solutions containing 50 mM of HTAC and 50 mM of NaSal, in the absence (Figure 1a) and presence of 5 g/l PEO (Figure 1b). Here, the

storage modulus, G', and loss modulus, G", are plotted logarithmically against log frequency ω at three temperatures; viz., 30, 40 and 50°C. Our previous study [24] found that the overlap concentration for PEO (M_w = 1 x 10^5 g/mol) is 10 g/l. Thus, the sample solutions shown in Figure 1b contain PEO below its overlap concentration. The measurements were made under controlled strain deformation in the linear viscoelastic region, at a strain $\gamma = 10\%$. When the temperature decreases below 15°C, the surfactant solution tends to precipitate, suggesting that the Krafft temperature for this HTAC/NaSal solution is below 15°C. Published data [14] shows that the threshold concentration separating the dilute and semidilute regimes for NaSal/HTAB solutions with the NaSal/HTAB mole ratio equal to unity occurs near [HTAB] = 10 mM, and is weakly dependent on temperature. Therefore, our sample solutions are well in the semidilute regime, in which the formation of wormlike micelles occurs.

Figure 1a indicates viscoelastic behavior typical of entangled wormlike solutions, consistent with literature data [4-10] for NaSal/HTAB solutions, featuring a terminal viscous flow regime at low frequencies, where $G' \sim \omega^{-2}$ and $G'' \sim \omega^{-1}$. There is a G' and G" crossover at a frequency $\omega_{co} = 1/\tau_R$, above which G' reaches the apparent plateau value, G_o, while G" decreases to a minimum, and then turns up, indicating the onset of a secondary relaxation mechanism. The crossover frequency, ω_{co}, and the frequency at the upturn of G" both shift to higher values with increasing temperature, but the magnitude of the upturn in G" diminishes as the temperature increases. Figure 1b shows that the results obtained from the solutions containing PEO are qualitatively similar, but that addition of PEO causes a significant decrease in the plateau modulus G_o, and a decrease in the crossover frequency, ω_{co}.

To clarify the differences between the two sets of data, we turn to Cole-Cole plots of the loss modulus, G", versus the storage modulus, G', plotted in Figures 2a and 2b for solutions in the absence and in the presence of PEO, respectively. Fits of the low frequency data to the Maxwell model (equations 3 and 4) are shown as solid lines. Evidently, at low frequencies, all the data sets follow closely the Maxwell behavior. However, at high frequencies, deviations from the osculating semicircle are observed, and at low temperatures, a minimum in G" can be seen at large G'. This

upturn has been interpreted as the transition to the Rouse or breathing regime [19, 25,26], and it moves out of the accessible frequency range at high temperatures. The diameter of the semicircle for NaSal/HTAC shows no systematic dependence on temperature, indicating a weakly temperature dependent plateau modulus, G_o in the temperature range examined (25 – 30°C). The solution containing PEO exhibits smaller semicircle diameters, indicating a substantial decrease in G_o compared to the solution without PEO. The different behaviors, manifested in comparing Figures 2a and 2b, clearly reflect the presence of a significant interaction between PEO and the NaSal/HTAC micelles on the solution rheology.

The influence of temperature on the characteristic parameters obtained via application of the Cates theory, for solutions without and with PEO addition, is tabulated in Tables 1 and 2. Values of τ_R computed as $\tau_R = \eta_o/G'_\infty$ are slightly smaller than $\tau_R = 1/\omega_{co}$ but show the same dependence on temperature, as well as HTAC and PEO concentration. From Table 1, the ratio $\zeta = \tau_{br}/\tau_{rep}$ increases for HTAC/NaSal from 0.057 at 25 °C to 0.59 at 50 °C, and, from Table 2, from 0.12 to >4 for HTAC/PEO/NaSal. This indicates that the dynamical behavior of these solutions falls in the dynamical crossover regime and evolves towards the slow-breaking limit, with increase of temperature. As can be seen from Table 1 and Table 2, η_o, τ_R, and $\overline{L}$ decrease strongly with temperature, whereas G_o and l_e are essentially temperature-independent in the range 25°C – 50°C. These observations are consistent with previous literature data for wormlike micelles [4-6, 12, 27-29]. For example, from the data of Shikata et al [4], for equimolar solutions of hexadecyltrimethylammonium bromide (HTAB) and NaSal, we interpolate a value $G'_\infty \sim 13.00$ Pa for 50 mM HTAB which compares remarkably well with our value $G'_\infty = 12.62$ Pa

Figure 3 plots the logarithm of the average micellar length, $\overline{L}$, the zero shear viscosity, η_o, and the stress relaxation time, τ_R ($\tau_R = \eta_o/G'_\infty$), versus the reciprocal of the absolute temperature for the HTAC/NaSal and the HTAC/NaSal/PEO solutions. Evidently, from Figure 3, each data set exhibits a linear dependence on 1/T, indicating Arrhenius behavior [28, 29]:

$$\tau_R = Ae^{E_a/RT} \tag{7}$$

$$\eta_0 = G'_\infty Ae^{E_a/RT} \tag{8}$$

where E_a is the flow activation energy, R is the gas constant, A is a pre-exponential factor, and G_o is the plateau modulus. From fits to these equations, the values of E_a are determined to be 24.92 and 22.74 kcal/mol for HTAC/NaSal and HTAC/NaSal/PEO, respectively. These values are comparable to the value (E_a = 25.40 kcal/mol) reported by Candau et al. [28] for HTAB in 0.25 M KBr brine. More cogent to this study, it is evident from Figure 3 that the addition of PEO results in substantial increases in $\overline{L}$, and τ_R, and relatively small changes in η_o.

Figure 4 presents the effect of PEO concentration on G'(ω) and G"(ω), when added to aqueous NaSal/HTAC solutions containing 50 mM HTAC and 50 mM NaSal at 30°C. The PEO concentration was varied from 1, 5 and 10 g/l. Note that the PEO concentration of 10 g/l corresponds to the estimated overlap concentration for our PEO of M_w = 1 x 10^5 g/mol. Figure 4 shows that G'(ω) and G"(ω) are very similar for PEO concentrations of 1 and 5 g/l, but that there is a significant increase in G'_∞ and ω_{co} when the PEO concentration is increased to 10 g/l. Reduced Cole-Cole plots (G''/G'_∞ versus G'/G'_∞) shown in Figure 5 indicate that G_o decreases substantially on addition of PEO up to 5 g/l, but then increases again at 10 g/l. Analysis of the data according to the Cates theory generates data on the effect of PEO concentration of the various parameters, G_o, G'_∞, η_o, τ_R, G''_{min}, l_e and $\overline{L}$ at 30°C which are listed in Table 2. Comparing Tables 1 and 2, the plateau modulus, G'_∞, shows a substantial decrease from 12.62 Pa to 8.33 Pa and 8.83 Pa, for PEO concentrations of 1 and 5 g/l, respectively then an increase to 12.0 Pa for 10 g/l PEO. The changes in G'_∞ are accompanied by an increase in τ_R from 0.63 s to 0.79 s up to 5 g/l PEO, and then a substantial decrease to τ_R = 0.25 s at 10 g/l PEO, also manifested as a decrease in η_o from 5.08 Pa.s to 2.89 Pa.s. The average micellar length, $\overline{L}$, increases slightly from 1.94 μm to 2.05 μm at 5 g/l PEO and then decreases dramatically to 1.27 μm at 10 g/l. Thus, of the three possibilities alluded to earlier, it is clear that addition of PEO at concentrations below the overlap value

results in the second outcome, i.e. a decrease in elasticity. Moreover, PEO at the overlap concentration causes a large decrease in viscosity and begins to rebuild the elasticity. We regard these observations as strong evidence that PEO disrupts the wormlike micellar network through complexing with HTAC micelles at PEO concentrations below the overlap value, and then, at the overlap concentration, PEO, complexed to HTAC micelles, begins to build its own space-filling network.

The effect of surfactant concentration on the rheology of HTAC/NaSal and HTAC/NaSal/PEO solutions was studied at fixed mole ratio of NaSal to HTAC of unity (Figures 6a and 6b). G'(ω) and G"(ω) were measured at 30°C, and the HTAC concentration was varied from 25, 50 and 100 mM. In Figure 6b, the PEO concentration was fixed at 5 g/l. Considering the data in the absence and in the presence of PEO, Figure 6a and 6b indicate that the plateau modulus, G_o, and the cross over frequency, ω_{co}, both increase substantially with HTAC concentration. Likewise, the frequency where the upturn in G" occurs also increases with increasing HTAC concentration. The reduced Cole-Cole plots of these data in Figure 7a and 7b demonstrate that there is an evolution from slow-breaking limit ($\zeta = \tau_{br}/\tau_{rep} \approx 1$) to fast breaking behavior ($\tau_{br}/\tau_{rep} << 1$), with increasing HTAC concentration, as manifested by the improved semicircular fit to the Maxwell model. This result is consistent with literature data [24].

Analysis of the data yields values of the rheological parameters: G_o, G'_∞, η_o, τ_R, l_e and $\overline{L}$ which are listed in Table 1 for HTAC/NaSal and in Table 2 for HTAC/NaSal/PEO solutions. The results indicate that addition of PEO produces a decrease in G_o and η_o for all three HTAC concentrations, whereas τ_R increases on adding PEO at HTAC concentrations of 25mM and 50mM, but slightly decreases at 100 mM.

7.5 Discussion and Conclusions

The dependence of temperature and HTAC concentration on the rheological properties of entangled, wormlike HTAC/NaSal solutions was investigated and the

results compared with those for HTAC/NaSal solutions to which PEO was added. The results for equimolar aqueous HTAC/NaSal solutions are consistent with literature data. G'(ω) and G"(ω) exhibit a low frequency behavior consistent with the theoretical prediction for a transient network of living polymers. With increasing HTAC concentration, the data show an evolution from dynamics characteristic of the slow breaking regime, where the wormlike micelle breaking time, τ_{br}, is comparable to the reptation time, τ_{rep}, to the fast breaking regime, where $\tau_{br} << \tau_{rep}$. At high frequencies, a minimum in G" ($G"_{min}$) indicates the appearance of Rouse relaxation modes with time scales corresponding to that of molecular motions between entanglements. The plateau modulus, G'_{∞}, and entanglement length, l_e, are temperature independent, while the stress relaxation time τ_R, zero shear viscosity, η_o and average micellar length, $\bar{L}$, each decrease strongly with increasing temperature. With increase of HTAC concentration, G'_{∞} increases significantly (l_e decreases), while τ_R decreases and η_o increases. $\bar{L}$ decreases with increasing HTAC concentration.

The addition of PEO, at concentrations well below the PEO overlap concentration, results in a substantial decrease of G_{∞} (increase of l_e) and an increase in τ_R and $\bar{L}$, so that η_o changes only slightly. Considering the three potential outcomes mentioned earlier, these observations are consistent with the second possibility that the binding of surfactant to PEO results in a decrease in the effective number of surfactant molecules that contribute to the entanglement network of wormlike micelles. Specifically, at T = 30 °C, light scattering analysis indicates a binding ratio of 0.68 g HTAC/g PEO [22]. Abstraction of the corresponding amount of HTAC from the HTAC/NaSal network represents a decrease in concentration available to the network of 20%, which would result in a decrease in modulus of 40%, assuming a concentration dependence $G'_{\infty} \sim c^{2.2}$ [4], which is reasonably consistent with our observed decrease of 30%. Note that the plateau modulus of HTAB/NaSal micelles is known to remain unchanged when NaSal is present in excess molar amounts [4]. When the PEO concentration is increased to 10 g/l in 50 mM HTAC (NaSal + HTAC concentration = 23.95 g/l), the change in G'_{∞} from the solution without PEO becomes negligible, but both τ_R and η_o decrease substantially.

From G''_{min} we further deduce that $\bar{L}$ decreases significantly. This distinct pattern of behavior further supports tha PEO disrupts the HTAC/NaSal micellar network, and, moreover, suggests that, at the PEO overlap concentration, PEO, bound with surfactant, begins to establish its own entanglement network.

7.6 Acknowledgements

S. Suksamranchit would like to acknowledge the financial support from the Thailand Research Fund (TRF), the RGJ grant no. PHD/0149/2543. This work was financially supported by the fund from MTEC, grant no. MT-43-POL-09-144-G, the funds from the ADB Consortium Grant, and the Conductive and Electroactive Polymer Research Unit of Chulalongkorn University. AMJ acknowledges financial support through NSF award DMR 0080114.

7.7 References

(1) Paasch, S.; Schambil, F.; Schwuger, J. *Langmuir* **1989**, 5, 1344.

(2) Wunderlich, I.; Hoffmann, H. *Rheol. Acta* **1987**, 26, 532

(3) Rehage, H.; Hoffmann, H. *J. Phys. Chem.* **1988**, 92, 4712

(4) Shikata, T.; Hirata, H.; Kotaka, T. *Langmuir* **1987**, 3, 1081.

(5) Shikata, T.; Hirata, H.; Kotaka, T. *Langmuir* **1988**, 4, 354.

(6) Shikata, T.; Hirata, H.; Kotaka, T. *Langmuir* **1989**, 5, 398.

(7) Clausen, T. M.; Vinson, P.K.; Minter, J.R.; Davis, H.T.; Talmon, Y.; Miller, W.G. *J. Phys. Chem.* **1992**, 96, 474.

(8) Hu, Y.; Wang, S.Q.; Jamieson, A. M. *J. Rheol.* **1993**, 37, 531.

(9) Hu, Y., Rajaram, C.V., Wang, S.Q., and Jamieson, A. M., *Langmuir*, **1994**, 10, 81.

(10) Hu, Y.; Wang, S.Q.; Jamieson, A. M., *J. Phys. Chem.*, **1994**, 98, 8555,

(11) Soltero, J.F.A., Puig, J.E., Manero, O., and Schulz, P.C., *Langmuir* **1995**, 11, 3337.

(12) Soltero, J.F.A and Puig, J. E. and Manero, O., *Langmuir* **1996**, 12, 2654.

(13) Kim, W. J.; Yang, S. M and Kim, M. *J. Colloid and Interface Sci.* **1997**, 194, 108.

(14) Kim, W. J and Yang, S. M. *J. Colloid and Interface Sci.* **2000**, 232, 225.

(15) Cates, M.S.; Candau, S. J. *J. Phys. Condens. Matter* **1990**, 2, 6869

(16) Cates, M. S. *Macromolecules* **1987**, 20, 2289.

(17) Cates, M. S.; Turner, M. *Europhys. Lett.* **1990**, 11, 681.

(18) Turner, M. S.; Cates, M. *Langmuir* **1991**, 7, 1590

(19) Granek, R.; Cates, M. E. *J. Chem. Phys.* **1992**, 96, 4758.

(20) See (a) Shashkina, Y.A.; Philippova, O.E.; Smirnov, V.A.; Blagodatskikh, I.V.; Churochkina, N.A.; Khokhlov, A.R. *Polymer Sci. Ser. A.* **2005**, 47, 1210; (b) Acharya , D.P.; Sato, T.; Kaneko, M.; Singh, Y.; Kunieda, H. *J. Phys. Chem. B* **2006**, 110, 754.

(21) Anthony, O.; Zana, R.; *Langmuir* **1994,** 10, 4048.

(22) Mya, K.Y.; Sirivat, A and Jamieson, A.M. *Macromolecules* **2001**, 34, 5260.

(23) Mya, K.Y.; Sirivat, A and Jamieson, A.M. *J. Phys. Chem B.* **2003**, 107, 5460.

(24) Suksamranchit, S.; Sirivat, A and Jamieson, A.M. *J. Colloid Interface Sci.*, **2005**, 294, 212

(25) Khatory, A.; Lequeux, H.; Kern, F.; Candau, S. J. *Langmuir* **1993**, 9, 1456.

(26) Kern, F.; Lequeux, F.; Zana, R.; Candau, S. J. *Langmuir* **1994**, 10, 1714.

(27) Srinivasa, R.; Eric, W. K. *Langmuir* **2001**, 17, 300.

(28) Candau, S. J.; Hirsch, E.; Zana, R.; Delsanti, M. *Langmuir* **1989**, 2, 1225.

(29) Fischer, P.; Rehage, H. *Langmuir* **1997**, 13, 7012.

(30) Mya, K.Y.; Sirivat, A and Jamieson, A.M. *Langmuir* **2000**, 16, 6131

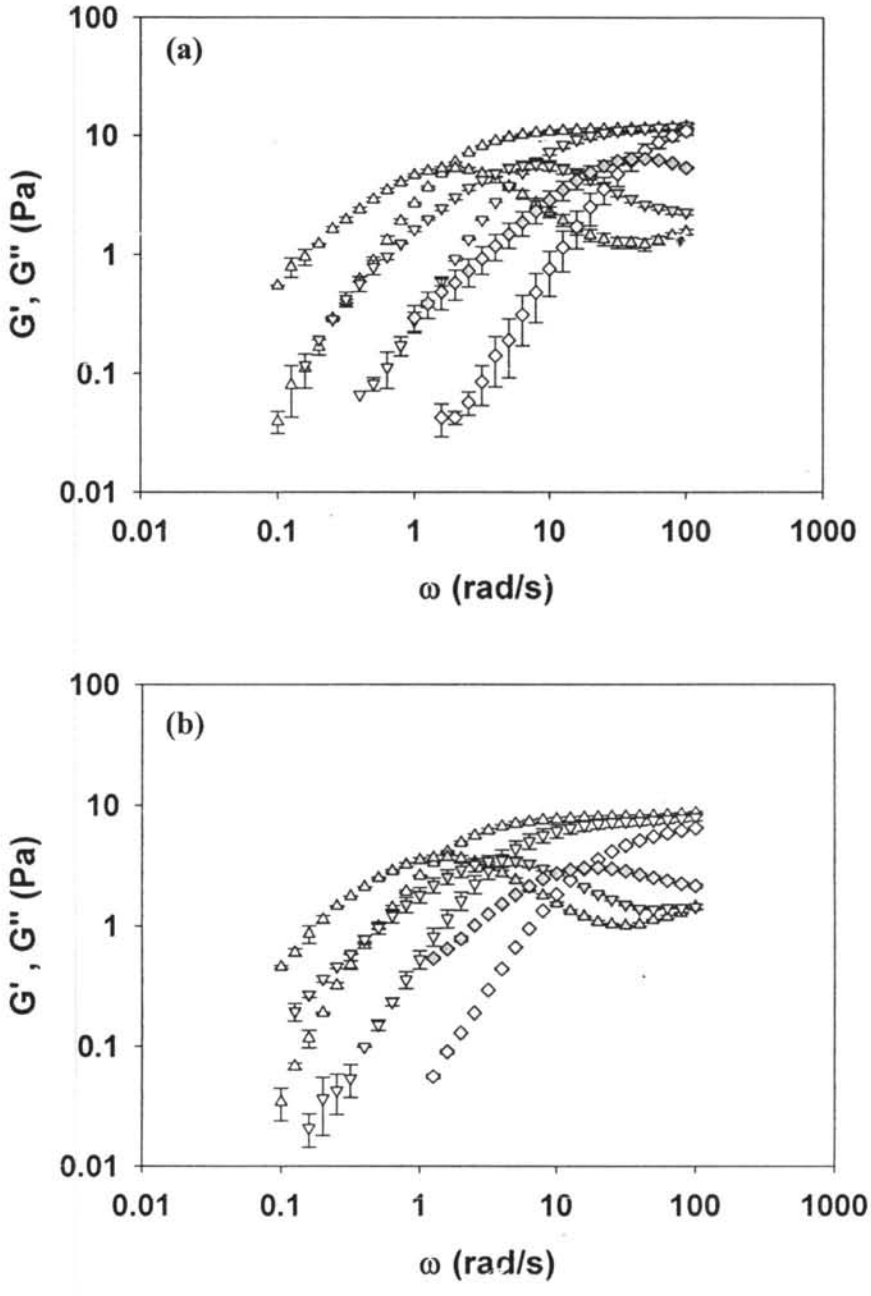

Figure 7.1 The effect of temperature on the frequency-dependent storage modulus, G'(ω) and loss modulus, G"(ω) is shown for aqueous solutions of HTAC 50 mM + NaSal 50 mM: **(a)** Without PEO and **(b)** With PEO 5 g/l: (△) G' at T = 30°C; (▲) G" at T = 30°C; (▽) G' at T = 40°C; (▼) G" at T = 40°C; (◇) G' at T = 50°C and (◆) G" at T = 50°C.

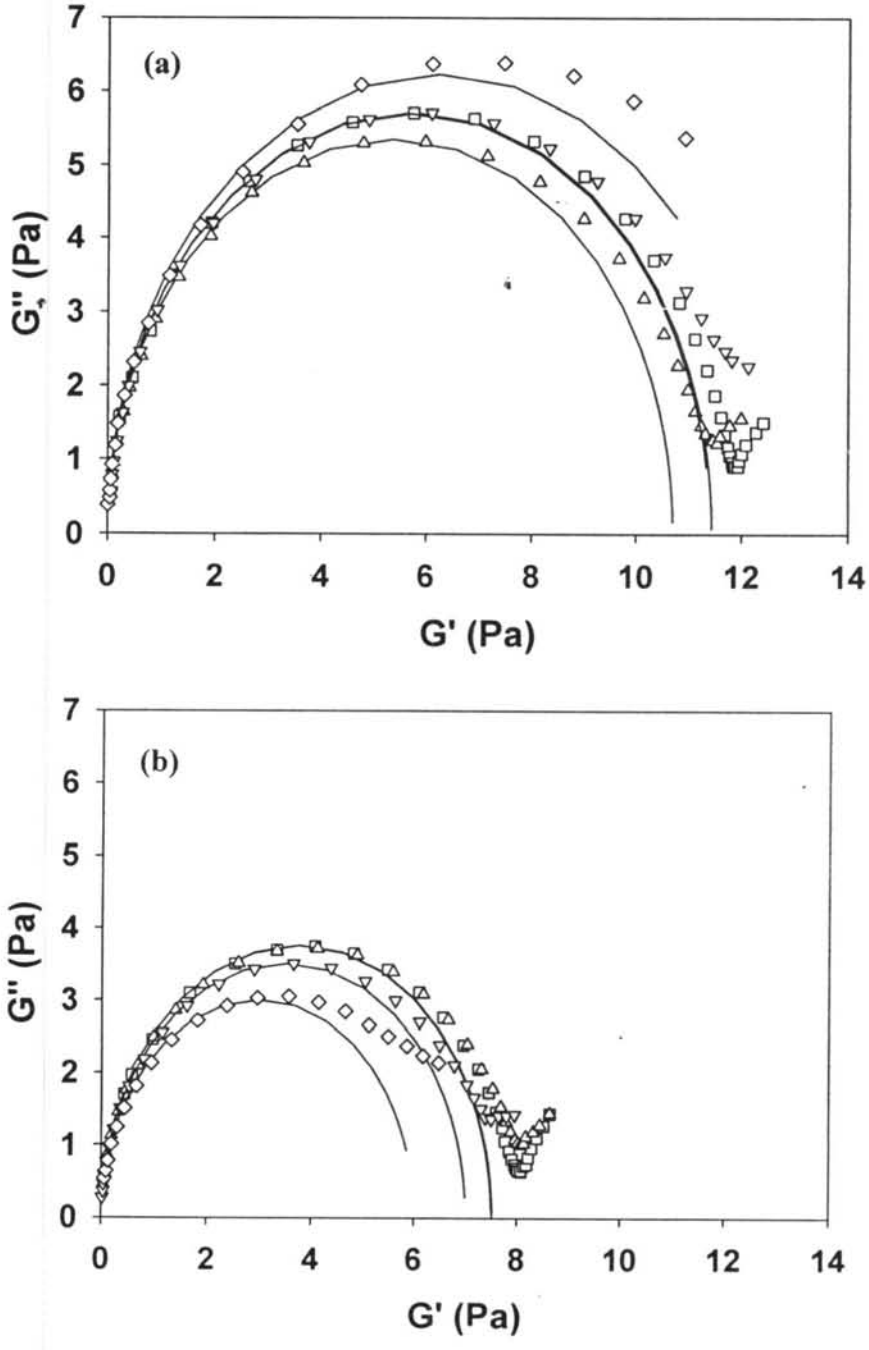

Figure 7.2 Cole-Cole plots of the loss modulus, G" versus the storage modulus, G' together with fits of the low-frequency data to the Maxwell model at different temperatures for aqueous solutions of HTAC 50 mM + NaSal 50 mM: **(a)** No PEO and **(b)** With PEO 5 g/l: (□) 25°C; (△) 30°C; (▽) 40°C and (◇) 50°C.

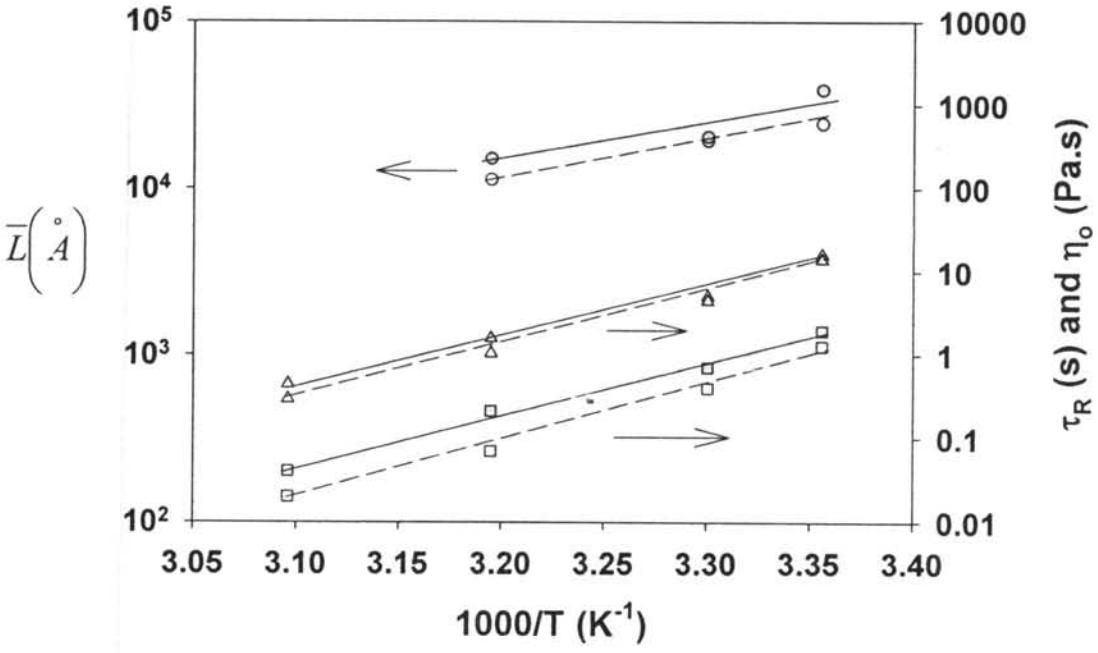

Figure 7.3 Semilogarithmic plot of the average micellar length, $\overline{L}$ (circle), the stress relaxation time, ($\tau_R = 1/\omega_{c\upsilon}$) (square) and the zero shear viscosity, η_o (triangle) versus 1000/T for the aqueous solutions of HTAC 50 mM + NaSal 50 mM:
(○, □, △) Without PEO and (●, ■, ▲) With PEO 5 g/l.

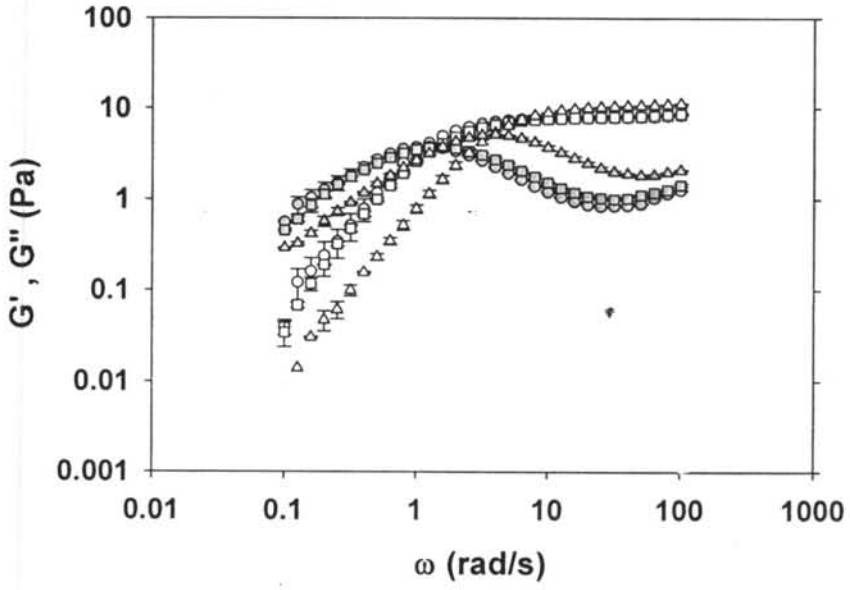

Figure 7.4 Dependence of storage modulus, G' and loss modulus, G" on frequency, ω at different PEO concentrations for aqueous solutions of HTAC 50 mm + NaSal 50 mM + PEO of M_w 1 x 10^5 g/mol at 30°C: (○) G' for PEO 1 g/l; (●) G" for PEO 1 g/l ; (□) G' for PEO 5 g/l; (■) G" for PEO 5 g/l; (△) G' for PEO 10 g/l and (▲) G" for PEO 10 g/l.

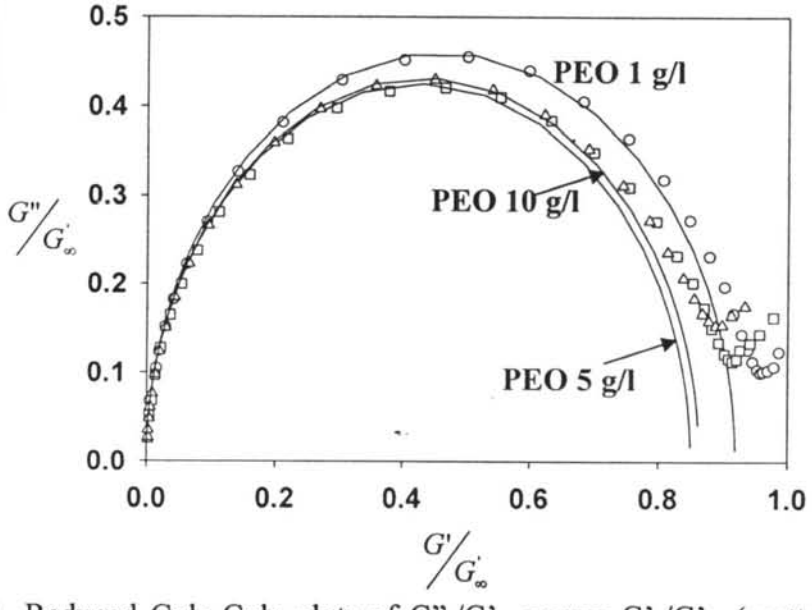

Figure 7.5 Reduced Cole-Cole plots of G" /G'$_\infty$ versus G' /G'$_\infty$ (scatter) together with low-frequency fits to the Maxwell model at different PEO concentrations for aqueous solutions containing 50 mM HTAC + 50 mM NaSal + PEO of M_w 1 x 10^5 g/mol at 30°C: (○) PEO 1 g/l; (□) PEO 5 g/l and (△) PEO 10 g/l.

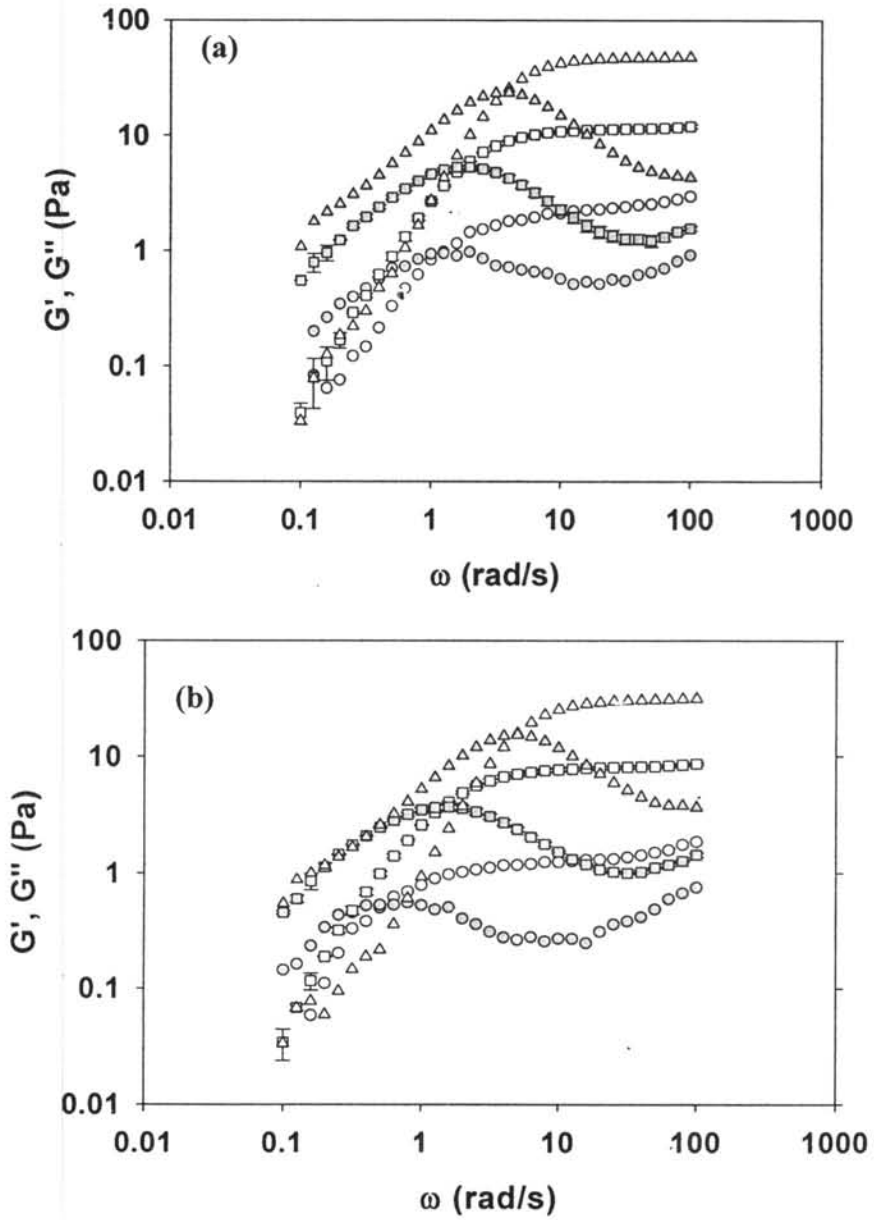

Figure 7.6 Effect of HTAC concentration on G'(ω) and G"(ω) for aqueous solutions containing equimolar amounts of HTAC and NaSal at 30°C:
(a) No PEO and **(b)** With 5 g/l PEO of M_w = 1 x 10^5 g/mole: (○) G' for HTAC 25 mM; (●) G" for HTAC 25 mM; (□) G' for HTAC 50 mM; (■) G" for HTAC 50 mM; (△) G' for HTAC 100 mM; and (▲) G" for HTAC 100 mM.

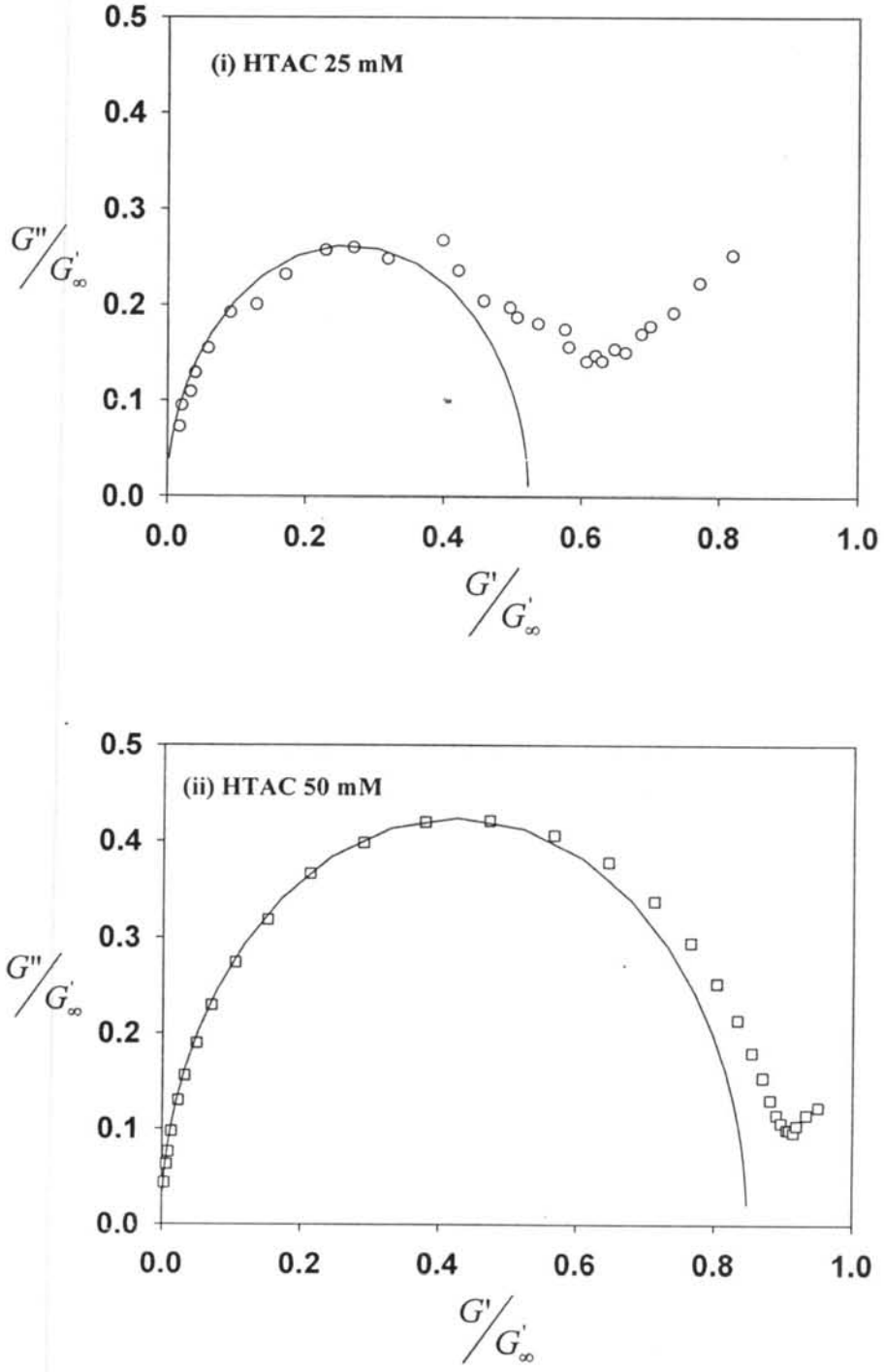

Figure 7.7a

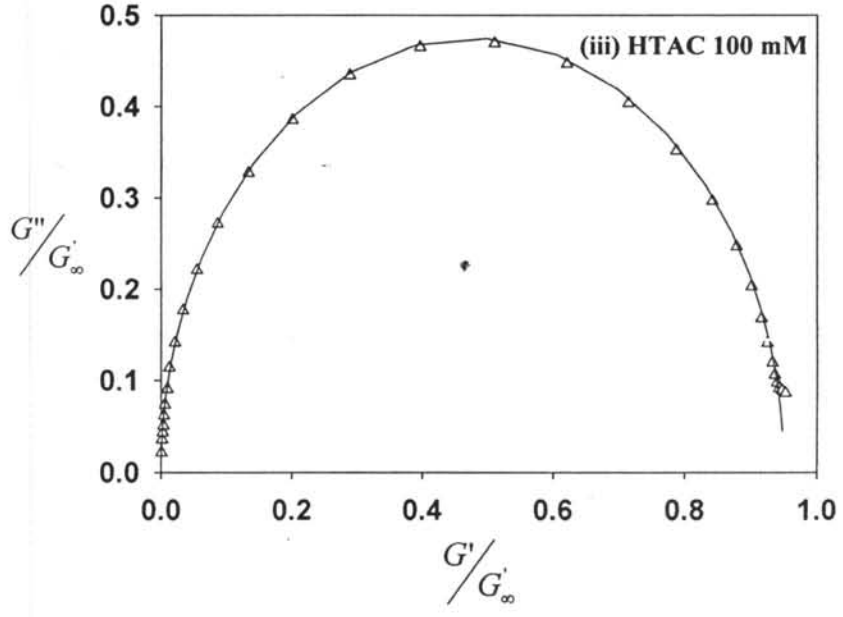

Figure 7.7a

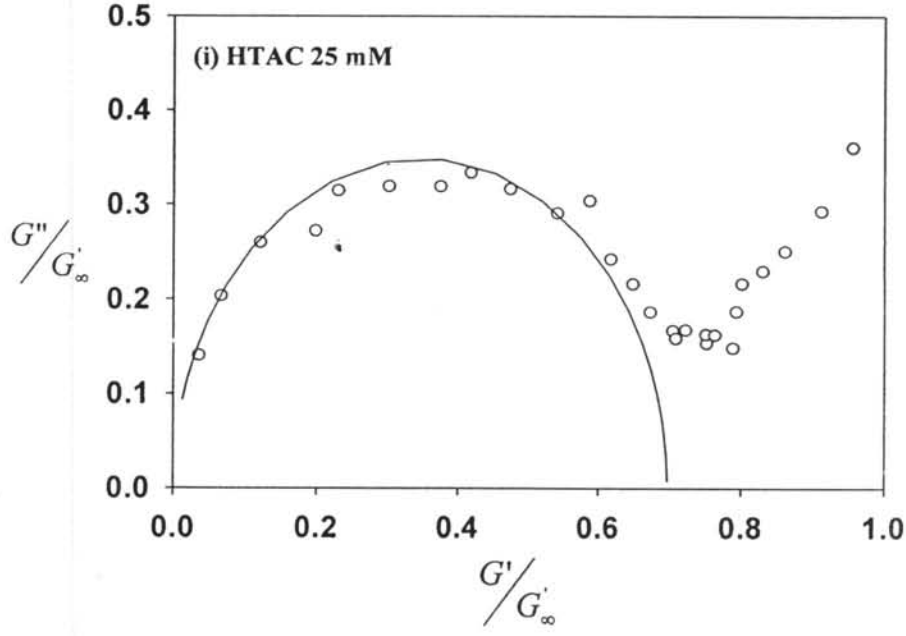

Figure 7.7b

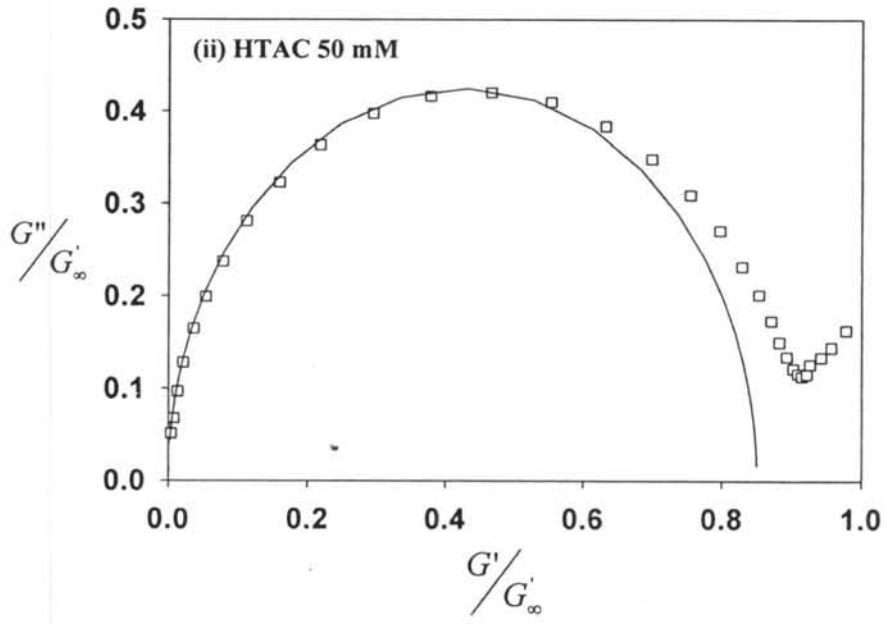

Figure 7.7b

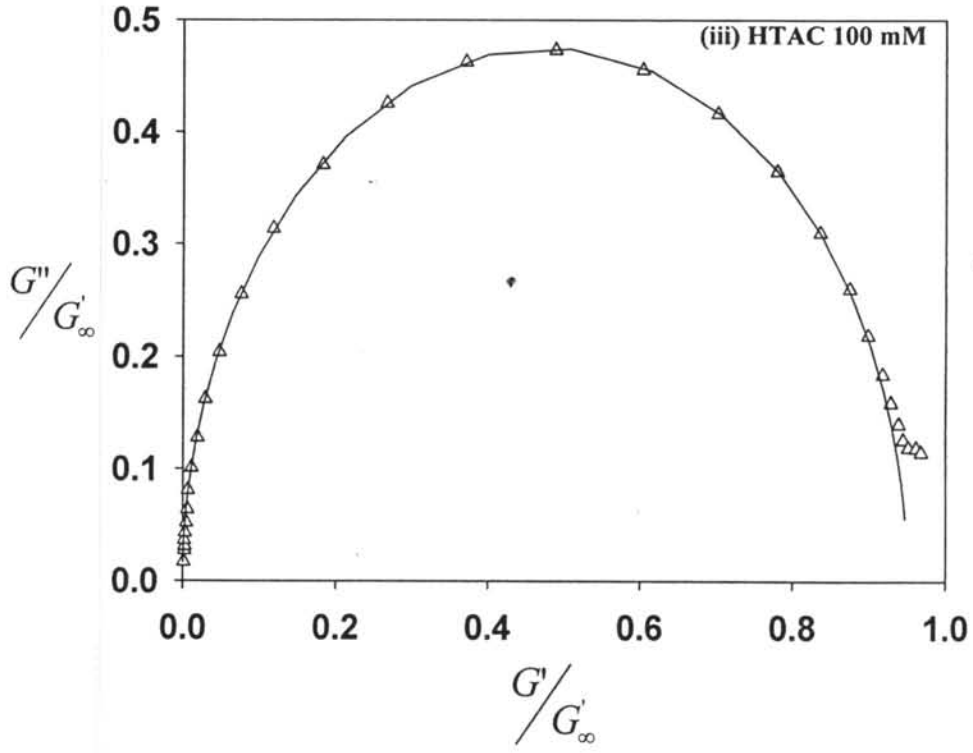

Figure 7.7 Reduced Cole-Cole plots of G" /G'$_\infty$, versus G' /G'$_\infty$ (scatter) together with fits to the Maxwell model at different HTAC concentrations for equimolar NaSal/HTAC solutions without and with PEO of M_w = 1 x 10^5 g/mol at 30°C: **(a)** No PEO and **(b)** With 5 g/l PEO: (i) HTAC = 25 mM; (ii) HTAC 50 mM and (iii) HTAC 100 mM.

Table 7.1 Dependence of Temperature and HTAC concentration on various parameters determined from the analysis of rheological data for aqueous solutions of HTAC + NaSal without PEO where the mole ratio of [NaSal]/[HTAC] = 1

T (°C)	HTAC (mM)	G_o (Pa)	G'_∞ (Pa)	G''_{min} (Pa)	DFS $=G_o/G'_\infty$	$\bar{\zeta}$	η_o (Pa.s)	$^a\tau_R$ (s)	$^b\tau_R$ (s)	τ_{br} (s)	τ_{rep} (s)	l_e (μm)	$\bar{L}$ (μm)
25	50	11.44	12.68	0.97	0.90	0.24	16.1	1.59	1.27	0.38	6.65	0.188	2.46
30	25	1.90	3.63	0.57	0.52	>2	1.71	0.79	0.47	>1.58	< 0.39	0.382	2.43
30	50	10.70	12.62	1.22	0.85	0.38	5.08	0.63	0.40	0.24	1.66	0.188	1.94
30	100	47.48	50.0	4.45	0.95	0.11	10.51	0.25	0.21	0.028	2.23	0.088	0.989
40	50	11.40	14.0	2.27	0.81	0.50	1.04	0.13	0.07	0.065	0.26	0.183	1.13
50	50	12.46	16.34	-	0.76	0.78	0.29	0.03	0.02	0.023	0.039	0.170	-

$^a\tau_R = 1/\omega_{co}$, $^b\tau_R = \eta_o / G'_\infty$; $\bar{\zeta} = \tau_{br}/\tau_R$

$\bar{L}$ = average micellar length; η_o = zero shear viscosity

G_{min} = the value of G" at the dip from Cole-Cole plot;

l_e = entanglement length

Table 7.2 Dependence of Temperature, PEO concentration and HTAC concentration on various parameters determined from the analysis of rheological data for aqueous solutions of HTAC + NaSal + PEO where the mole ratio of [NaSal]/[HTAC] = 1

T (°C)	HTAC (mM)	PEO (g/l)	G_o (Pa)	G'_∞ (Pa)	G''_{min} (Pa)	DFS $=G_o/G'_\infty$	$\bar{\varsigma}$	η_o (Pa.s)	$^a\tau_R$ (s)	$^b\tau_R$ (s)	τ_{br} (s)	τ_{rep} (s)	l_e (μm)	$\bar{L}$ (μm)
25	50	5	7.52	8.69	0.63	0.86	0.34	17.02	2.51	1.96	0.86	7.33	0.284	3.91
30	25	5	1.16	1.66	0.26	0.70	1.21	1.43	1.58	0.86	1.92	1.32	0.587	3.75
30	50	1	7.66	8.33	0.84	0.92	0.17	5.88	0.79	0.71	0.13	4.80	0.240	2.38
30	50	5	7.51	8.83	1.00	0.85	0.38	4.50	0.79	0.51	0.30	2.08	0.232	2.05
30	50	10	10.36	12.0	1.84	0.86	0.34	2.89	0.25	0.24	0.085	0.73	0.195	1.27
30	100	5	30.70	32.3	3.71	0.95	0.11	5.62	0.20	0.17	0.022	1.82	0.113	0.98
40	50	5	7.01	8.69	1.37	0.81	0.5	1.58	0.25	0.18	0.125	0.5	0.238	1.51
50	50	5	6.00	11.4	-	0.53	>2	0.44	0.06	0.04	>0.12	< 0.03	0.209	-

$^a\tau_R = 1/\omega_{co}$, $^b\tau_R = \eta_o / G'_\infty$

$\bar{\varsigma} = \tau_{br}/\tau_R$; $\bar{L}$ = average micellar length

η_o = zero shear viscosity ; G_{min} = the value of G" at the dip from Cole-Cole plot

l_e = entanglement length